



Published in final edited form as:

Nat Commun. ; 6: 6804. doi:10.1038/ncomms7804.

Association of *CLEC16A* with human common variable immunodeficiency disorder and role in murine B cells

Jin Li^{1,*}, Silje F. Jørgensen^{2,*}, S. Melkorka Maggadottir^{1,3,*}, Marina Bakay¹, Klaus Warnatz⁴, Joseph Glessner¹, Rahul Pandey¹, Ulrich Salzer⁴, Reinhold E. Schmidt⁵, Elena Perez⁶, Elena Resnick⁷, Sigune Goldacker⁴, Mary Buchta⁴, Torsten Witte⁵, Leonid Padyukov⁸, Vibeke Videm⁹, Trine Folseraas^{2,10}, Faranaz Atschekzei⁵, James T. Elder^{11,12}, Rajan P. Nair¹¹, Juliane Winkelmann^{13,14,15,16}, Christian Gieger¹⁷, Markus M Nöthen^{18,19}, Carsten Büning²⁰, Stephan Brand²¹, Kathleen E. Sullivan^{3,22}, Jordan S. Orange²³, Børre Fevang^{2,24}, Stefan Schreiber²⁵, Wolfgang Lieb²⁶, Pål Aukrust^{2,24}, Helen Chapel²⁷, Charlotte Cunningham-Rundles⁷, Andre Franke²⁵, Tom H. Karlsen^{2,10,28}, Bodo Grimbacher⁴, Hakon Hakonarson^{1,29,#,□}, Lennart Hammarström^{30,#}, and Eva Ellinghaus^{25,#}

¹Center for Applied Genomics, Children's Hospital of Philadelphia, Philadelphia, USA

²K.G. Jebsen Inflammation Research Centre, Research Institute of Internal Medicine, Division of Cancer Medicine, Surgery and Transplantation, Oslo University Hospital, Rikshospitalet, Oslo, Norway

³Division of Allergy and Immunology, The Children's Hospital of Philadelphia, Philadelphia, Pennsylvania, USA

⁴Center for Chronic Immunodeficiency (CCI), University Medical Center Freiburg and, University of Freiburg, Freiburg, Germany

⁵Clinic for Immunology and Rheumatology, Hannover Medical School, Hannover, Germany

⁶Division of Pediatric Allergy and Immunology, University of Miami Miller School of Medicine, Miami, Florida, USA

⁷Institute of Immunology and Department of Medicine, Mount Sinai School of Medicine, New York, USA

Users may view, print, copy, and download text and data-mine the content in such documents, for the purposes of academic research, subject always to the full Conditions of use:http://www.nature.com/authors/editorial_policies/license.html#terms

□ **Correspondence to:** Prof. Hakon Hakonarson, MD, PhD, Director, Center for Applied Genomics, Children's Hospital of Philadelphia, Abramson Research Center Suite 1216, 3615 Civic Center Blvd, Philadelphia, PA 19104, United States, hakonarson@email.chop.edu.

*These authors contributed equally to this work

#These authors jointly supervised this work

AUTHOR CONTRIBUTIONS

JL, SFJ, MM, MB, JG, RP and EE performed data and statistical analysis. KW, JG, US, RES, EP, ER, SG, MB, TW, LP, VV, TF, FA, JTE, RPN, JW, CJ, MMN, CB, SB, KS, JSO, BF, SS, WL, PA, HC, CCR, AF, THK, BG, HH and LH contributed to the ascertainment of affected individuals and/or sample and clinical data collection. THK, HH, LH and EE coordinated and supervised the project. JL, SFJ, MM, PA, THK and HH drafted the manuscript. All authors revised the manuscript for critical content and approved of the final version.

COMPETING FINANCIAL INTEREST

The authors declare no competing interest.

- ⁸Rheumatology Unit, Department of Medicine, Karolinska Institutet and Karolinska University Hospital Solna, Stockholm, Sweden
- ⁹Department of Laboratory Medicine, Children's and Women's Health, Norwegian University of Science and Technology. Trondheim, Norway
- ¹⁰Norwegian PSC Research Center, Division of Cancer, Surgery and Transplantation, Oslo University Hospital, Oslo, Norway
- ¹¹Department of Dermatology, University of Michigan, Ann Arbor, Michigan, USA
- ¹²Ann Arbor Veterans Affairs Hospital, Ann Arbor, Michigan, USA
- ¹³Institute of Human Genetics, Helmholtz Center Munich, German Research Center for Environmental Health, Neuherberg, Germany
- ¹⁴Department of Neurology, MRI, Technische Universität München, Munich, Germany
- ¹⁵Synery Munich Cluster for Systems Neurology
- ¹⁶Stanford University, Department of Neurology and Neurosciences and Center for Sleep Sciences and Medicine, USA
- ¹⁷Institute of Genetic Epidemiology, Helmholtz Center Munich, German Research Center for Environmental Health, Neuherberg, Germany
- ¹⁸Institute of Human Genetics, University of Bonn, Bonn, Germany
- ¹⁹Department of Genomics, Life and Brain Center, University of Bonn, Bonn, Germany
- ²⁰Department of Hepatology and Gastroenterology, Charité, Campus Mitte, Berlin, Germany
- ²¹Department of Medicine II–Grosshadern, Ludwig-Maximilians-University (LMU), Munich, Germany
- ²²Department of Pediatrics, The Perelman School of Medicine, University of Pennsylvania, Philadelphia, Pennsylvania, USA
- ²³Section of Immunology, Allergy, and Rheumatology, Department of Pediatric Medicine, Texas Children's Hospital, Houston, TX, USA
- ²⁴Section of Clinical Immunology and Infectious diseases, Oslo University Hospital Rikshospitalet, Norway
- ²⁵Institute of Clinical Molecular Biology, Christian-Albrechts-University Kiel, Germany
- ²⁶Institute of Epidemiology and Biobank popgen, Christian-Albrechts-University of Kiel, Kiel, Germany
- ²⁷Department of Clinical Immunology, Nuffield Department of Medicine, University of Oxford, UK
- ²⁸Institute of Clinical Medicine, University of Oslo, Oslo, Norway
- ²⁹Division of Human Genetics, The Children's Hospital of Philadelphia, Philadelphia, Pennsylvania, USA
- ³⁰Department of Laboratory Medicine, Division of Clinical Immunology and Transfusion Medicine, Karolinska University Hospital, Huddinge, Stockholm, Sweden

Abstract

Common variable immunodeficiency disorder (CVID) is the most common symptomatic primary immunodeficiency in adults, characterized by B cell abnormalities and inadequate antibody response. CVID patients have considerable autoimmune comorbidity and we therefore hypothesized that genetic susceptibility to CVID may overlap with autoimmune disorders. Here, in the largest genetic study performed in CVID to date, we compare 778 CVID cases with 10,999 controls across 123,127 single nucleotide polymorphisms (SNPs) on the Immunochip. We identify the first non-HLA genome-wide significant risk locus at *CLEC16A* (rs17806056, $P=2.0\times 10^{-9}$) and confirm the previously reported human leukocyte antigen (HLA) associations on chromosome 6p21 (rs1049225, $P=4.8\times 10^{-16}$). *Clec16a* knock down (KD) mice showed reduced number of B cells and elevated IgM levels compared to controls, suggesting that *CLEC16A* may be involved in immune regulatory pathways of relevance to CVID. In conclusion, the *CLEC16A* associations in CVID represent the first robust evidence of non-HLA associations in this immunodeficiency condition.

Introduction

Common variable immunodeficiency (CVID) has a prevalence of approximately 1 in 25,000 in European populations. Recurrent bacterial respiratory tract infections constitute the predominant clinical manifestation, but a subset of CVID patients also develops gastrointestinal manifestations and lymphoid hyperplasia. In addition, various forms of autoimmune disorders affect up to 25% of the patients, of which the most common is autoimmune thrombocytopenia¹. The immunological hallmark of CVID is the B cell defect with inability to produce adequate antibody responses, but patients also show other immunological abnormalities such as T cell dysfunction, monocyte/macrophage hyperactivity and signs of low-grade systemic inflammation².

The focus of CVID genetics over the years has largely been to determine the presence of monogenic subtypes, leading to the identification of familial affection of a series of immunodeficiency genes, including *CD19*³, *CD20*⁴, *CD81*⁵, *CR2*⁶, *ICOS*⁷, *LRBA*⁸, *PLCG2*⁹, *PRKCD*¹⁰ and *TNFRSF13B*¹¹. However, most of the CVID cases are sporadic and although formal heritability estimates have not been made, a complex model of inheritance likely accounts for the majority of patients¹². The human leukocyte antigen (HLA) haplotype association with CVID was found earlier by tissue typing¹³ and a recent genome-wide association study in CVID further supports a complex genetic heritability in CVID, with common variants within HLA complex associating with disease development¹⁴. To what extent common genetic variations outside this region contribute to CVID susceptibility is unknown.

We hypothesize that the autoimmune comorbidity in CVID may occur on the basis of shared genetic susceptibility. We perform dense autoimmune risk loci genotyping on the Immunochip in 778 CVID cases and 10,999 controls, representing the largest CVID study panel investigated for genetic risk factors to date. We identify a novel non-HLA risk locus at *CLEC16A* and replicate the previously reported HLA associations at chromosome 6p21. In *Clec16* knock-down mice, we found a reduced proportion of B cells and elevated IgM

secretion, pointing to a role of *CLEC16A* in B cell function of potential relevance to CVID and other *CLEC16A* associated conditions.

Results

A novel CVID susceptibility locus harboring *CLEC16A*

To systematically assess established autoimmune risk loci for associations in CVID, we genotyped 886 CVID cases and 11,552 controls of European ancestry from Scandinavia, Germany, United Kingdom and the United States (Table 1, Supplementary Table 1 and Supplementary Fig. 1) using the Immunochip, a targeted genotyping array with dense single nucleotide polymorphism (SNP) coverage across 186 known disease loci from 12 immune-mediated diseases¹⁵. Following standard quality control measures, a total of 123,127 SNPs with a minor allele frequency greater than 1% from 778 cases and 10,999 controls remained available for analysis. Association testing was performed using logistic regressions with the first three principal components as covariates to adjust for population structure (residual genomic inflation factor $\lambda=1.04$) (Supplementary Fig. 2 and Supplementary Fig. 3).

On chromosome 16p13.13, we detected 22 genome wide significant ($P < 5 \times 10^{-8}$) SNPs spanning the *CLEC16A* locus in our logistic regression analysis. The most strongly associated SNP (rs17806056, $P = 2.0 \times 10^{-9}$) was located in intron 19 of *CLEC16A* (Table 2, Fig. 1a and Fig. 1b). An additional 15 imputed SNPs also showed genome wide significance (Supplementary Table 2). Conditioning on SNP rs17806056, significant associations of other *CLEC16A* SNPs were ablated, suggesting that the SNP is representative of a single association signal at *CLEC16A*. *CLEC16A* encodes a protein belonging to the C-type lectin-like domain family and is expressed in dendritic cells, natural killer cells and B cells^{16, 17}. Stratified analysis also suggested that *CLEC16A* variants may correlate with several clinical subtypes and immunological phenotypes in CVID (e.g. lymphoid hyperplasia) and not just the autoimmune subtype (Supplementary Table 3), although none of these associations were robust at the genome-wide significance level.

We conducted quantitative real-time polymerase chain reaction (qRT-PCR) on blood from CVID cases to investigate whether there is any correlation between *CLEC16A* expression and the rs17806056 genotype. Statistically significant higher level of *CLEC16A* mRNA was detected in the AA group which carries two copies of the minor allele, compared to the TT group (Fig. 1c). We did not find any significant difference in mRNA levels of the neighboring *SOCS1* or *DEXI* genes according to rs17806056 genotype status (Supplementary Fig. 4). We further assessed annotations from the ENCODE¹⁸ project for all CVID associated SNPs within the 16p13.13 region (Supplementary Table 4). Of note, several of the CVID associated SNPs (rs36110069, rs35300161, rs2867880, rs7203459 and rs34972832) are predicted to affect binding sites for the GATA2 transcription factor where binding to SNP rs34972832 and neighboring sequences is detected in the human K562 leukemia cell line¹⁸. GATA2 is also involved in different adult immunodeficiency state (monoMAC syndrome)¹⁹. Further studies are warranted to explore the relevance of these observations in vivo.

Clec16 knock-down affects murine B-cells

Whereas *CLECI6A* is highly expressed in human B cells, a role of *CLECI6A* in these cells has not been established. Given the paramount importance of B cell defects in CVID development, we explored the biological implications of *Clec16a* knock down (KD) in murine B cells isolated from splenocytes. We detected a 54.4% ($\pm 8.4\%$) reduction of the total number of CD19+ B cells in the splenocyte population after induction of *Clec16a* KD using tamoxifen, when compared to non-tamoxifen-treated littermates (control group) ($P=6.25\times 10^{-6}$ in two-sided T-test). In particular, the fraction of CD19+ B cells in splenocytes is reduced ($17.4\% \pm 5.0\%$, $P=2.45\times 10^{-3}$ in two-sided T-test) (Fig. 2a and Supplementary Table 5). We did not detect significant differences in the fraction of CD27+ cells, or for B cell proliferation assaying (MTT). However, B cells from *Clec16a* deficient mice exhibited an altered immunoglobulin profile as compared with control mice with increased levels of IgM ($P = 0.003$ in two-sided T-test), but no changes in serum levels of IgG and IgA (Fig. 2b). In sum, the supplementary murine Clec16a data suggest an impact of *CLECI6A* on B cell function.

Candidate gene association statistics

In addition to the genome-wide significant *CLECI6A* locus, we also found six loci exhibiting suggestive evidence for association ($5\times 10^{-8} < P\text{-value} < 5\times 10^{-5}$) (Supplementary Fig. 5 and Supplementary Table 6). Although replication in future study panels is required for formally establishing these loci (*FCRLA*, *EOMES*, *TNIP1*, *TNFAIP3*, *TNFSF11* and *PTPN2*) in CVID, prior probability for genuine association is enhanced by findings in other immune-mediated diseases (Supplementary Table 6). Furthermore, SNPs at four genes previously suggested to be involve in familial CVID subtypes, *CR2*, *ICOS*, *MSH5* and *TNFRSF13B*, showed nominally significance association ($P < 0.05$) in the present analysis (Supplementary Table 7).

HLA-DQB1 associations

In line with previous studies¹⁴ we detected strong associations with SNPs within the HLA complex on chromosome 6p21, peaking at rs1049225 in the 3' UTR of *HLA-DQB1* ($P=4.8\times 10^{-16}$) (Table 2, Fig. 1a and Supplementary Fig. 6). By stepwise conditional logistic regressions we found that the association signal consists of multiple independent effects (Supplementary Table 8 and Supplementary Fig. 7). We imputed classical *HLA-A*, *HLA-C*, *HLA-B*, *HLA-DRB1*, *HLA-DQB1*, *HLA-DQA* and *HLA-DPBI* alleles (Supplementary Table 9), revealing *HLA-DQB1* associations with HLA-DQB1*02:01 and *05:03 (risk alleles) as well as HLA-DQB1*06:02 and DQB1*06:03 (protective alleles). Further studies involving direct sequencing of all HLA class I and II loci and determination of their protein structure and peptide binding profiles are required to further explore the link between these HLA haplotypes and CVID development. Of note for the present report, we found no statistical evidence for interaction between *CLECI6A* and the HLA associated risk to CVID (Supplementary Table 10).

Autoimmune disease associations at the *CLEC16A* locus

Genome-wide association studies have detected *CLEC16A* associations in multiple phenotypes ranging from prototypical autoimmune disorders (e.g. type 1 diabetes²⁰ and primary biliary cirrhosis²¹) via immune-mediated conditions driven by exogenous antigens (e.g. celiac disease²² and allergy²³) to suggestive associations ($P = 1.8 \times 10^{-7}$) observed in selective IgA deficiency²⁴. The majority of significant SNPs from these studies are trans-ethnic, localize to the same linkage disequilibrium (LD) block, and are in high to moderate LD with the most strongly associated SNP within *CLEC16A* in the current study (rs17806056) (Supplementary Table 11).

Discussion

The present study has demonstrated a potential role of *CLEC16A* in the pathogenesis of CVID by strong genetic associations and its involvement in murine B cell function.

Because of the prominent *CLEC16A* SNP associations in a variety of auto-immune diseases, several studies have been carried out to examine the biological function of *CLEC16A*. Its *Drosophila* homologue Ema has been found to localize to the endosomal and Golgi membranes^{25, 26}. Ema mutants show defects in lysosomal degradation and protein trafficking²⁵. It is also essential for autophagosomal growth and autophagy processes²⁶, which are of major importance for proper immune regulation, including regulation of inflammasome activation. *CLEC16A* is evolutionarily conserved and may rescue the *Drosophila* Ema mutant phenotypes^{25, 26}. Human *CLEC16A* has been reported to be abundantly expressed in dendritic cells, natural killer cells and B-cells^{16, 17}. Zouk and colleagues demonstrated, by using a human erythromyeloblastoid leukemia cell line, K562 cells, and human lymphoblastoid cell lines, that *CLEC16A* is localized with an endoplasmic reticulum marker and that knockdown of *CLEC16A* did not affect T-cell co-stimulation²⁷. Recent murine data indicated that Clec16a is localized at endosomal membrane and forms a protein-complex with Nrdp1 which is an E3 ubiquitin-protein ligase²⁸. Clec16a may thus regulate mitophagy through the Nrdp1/Parkin pathway²⁸. Adding to this existing knowledge, the present study has shown that *CLEC16A* may also be involved in B cell function. Although we could not reproduce the complete CVID phenotype in Clec16a KD B cells, findings strongly suggest that *CLEC16A*, in combination with other dysregulated pathways, may contribute to the B cell dysfunction observed in these patients.

The relationship of *CLEC16A* expression and its genotype status has been investigated. We have previously shown that *CLEC16A* is differentially expressed based on the risk allele, reported with the protective minor allele showing a higher expression than the risk allele²⁰ and a similar observation was made in the present study. The correlation is further complicated by the existence of three *CLEC16A* isoforms, which could lead to isoform specific correlations. Examining the relative expression level of the long isoforms vs. short isoform, a correlation with multiple sclerosis-associated SNP rs12708716 genotype status has been observed in human thymic tissues. However, no association was found when it was examined in whole blood²⁹. Therefore, the effect of SNP genotype status on *CLEC16A* expression could be both isoform-specific and cell-type/tissue-type dependent³⁰. Furthermore, the sample size in each study is small and may be underpowered to detect a

correlation. At this stage, though *CLEC16A* is a promising candidate gene to function in the pathogenesis of CVID as demonstrated in our study, we could not fully exclude the possibility that CVID associated SNPs in *CLEC16A* introns are tagging other proximal genes, although we find this is unlikely.

The identification of *CLEC16A* as a significant CVID risk locus reflects the notion that most genetic risk loci for immune-related diseases are pleiotropic. Significant overlap of risk loci between autoimmune disease and immune deficiency has also been found for those of rheumatoid arthritis³¹. The biological explanation of the overlap likely differs from locus to locus, but the overall interpretation is that of an imperfect relationship between clinical disease phenotyping and genetically determined pathophysiology. Importantly, the finding of *CLEC16A* associations in both autoimmunity, allergy and as given by the present study: an immunodeficiency condition, characterized by impaired immune response to certain capsulated bacteria, is particularly interesting, since the mechanisms leading to persistent immune activation and autoimmunity in CVID, is not clear. Our findings may suggest that altered function of *CLEC16A* could be “the missing link” between immunodeficiency and immune action in CVID. The current identification of novel, highly robust *CLEC16A* associations in CVID raises conceptually novel opportunities for exploring mechanisms underlying the autoimmune co-morbidity and the chronic inflammation observed in CVID. Hypothetically, the *CLEC16A* associated aspects of adult immunodeficiency states may reveal novel concepts for the basis of immune activation in autoimmunity.

In conclusion, we have identified the first genome-wide significant non-HLA CVID risk locus at *CLEC16A* in the largest genetic study performed in this disease to date. *CLEC16A* has previously been linked to autoimmune disorders and the fact that *Clec16a* deficient mice showed decreased number of B cells suggests that *CLEC16A* could represent a link between autoimmunity and immunodeficiency in CVID.

Methods

Study Subjects Description

Study Subjects were recruited from five countries: Sweden, Norway, USA, United Kingdom and Germany (Table 1 and Supplementary Table 1) The diagnosis of common variable immunodeficiency disorder (CVID) was defined as decreased serum levels (> 2 SD) of IgG, IgA and/or IgM and exclusion of other forms of hypogammaglobulinemia according to the WHO expert group on primary immunodeficiency and the International Union of Immunological Societies (IUIS)^{32, 33}. Controls were recruited from blood donors or population-based studies.

The Swedish CVID cases (n=93) were recruited at the Department of Laboratory Medicine, Division of Clinical Immunology and Transfusion Medicine, Karolinska University Hospital, Huddinge, Stockholm. The Swedish controls (n=2,096) were part of a population based case-control study named Epidemiological Investigation of Rheumatoid Arthritis (EIRA)³⁴.

The CVID patients in the Norwegian panel (n=112) were recruited from the Section of clinical Immunology and infectious diseases at Oslo University Hospital Rikshospitalet, Oslo, Norway. DNA samples from healthy Norwegian controls (n=1,405) were selected from the Norwegian Bone Marrow Donor Registry (NMBDR) and the North-Trøndelag Health Study (HUNT).

The CVID patients in the USA/UK panel (n=330) were recruited from 4 locations: the Immunodeficiency Clinic at Mount Sinai Medical Center, New York, NY, the Division of Allergy, Immunology and Rheumatology, All Children's Hospital, St Petersburg, FL, the Division of Allergy and Immunology at The Children's Hospital of Philadelphia, PA and the department of Clinical Immunology in the Nuffield Department of Medicine, Oxford Radcliffe Hospital, UK. All USA/UK cases were genotyped at the Center for Applied Genomics, Children's Hospital of Philadelphia, PA.

The USA controls (n=1402) were recruited at the University of Michigan and genotyped at the Institute of Clinical Molecular Biology, Christian-Albrechts-University of Kiel (as part of the PAGE Immunochip dataset³⁵).

The German CVID cases (n=351) were recruited at the Center for Chronic Immunodeficiency, University Hospital of Freiburg and at the Clinic for Immunology and Rheumatology, Hannover Medical School, Hannover. DNA from 2,696 German healthy controls was obtained through the Northern German biobank PopGen³⁶ (<http://www.popgen.de>) and the University Hospital Schleswig-Holstein. Genotyping of these 2,696 controls was performed at the Institute of Clinical Molecular Biology, Christian-Albrechts-University of Kiel. 1,924 German controls were part of an independent population-based sample from the general population living in the region of Augsburg (Cooperative Health Research in the Region of Augsburg (KORA)), southern Germany³⁷, and were genotyped at the Helmholtz Center in Munich. 1,500 German controls were recruited from the population-based epidemiological Heinz-Nixdorf Recall (HNR) study and genotyped at the Life and Brain Center at the University Clinic Bonn. 314 individuals were of south German ancestry and were part of the control population Munich recruited from the Bavarian Red Cross and 215 individuals were recruited from the Charité-Universitätsmedizin Berlin. These samples were genotyped at the University of Pittsburgh Genomics and Proteomics Core Laboratories.

The study was approved by the regional ethical review board in Stockholm, the regional committees for medical and health research ethics in Norway, Ethikkommission der Universitätsklinik Freiburg, Ethik-Kommission der Medizinische Hochschule Hannover, Ethik-Kommission der Medizinischen Fakultät der Christian-Albrechts-Universität zu Kiel and the Institutional Review Board of: Mount Sinai School of Medicine, the University of Oxford, the Children's Hospital of Philadelphia, and the University of South Florida. Written informed consent for blood sample collection, processing and genotyping were obtained by all participants.

ImmunoChip genotyping

DNA samples were genotyped using the ImmunoChip, an Illumina iSelect HD custom genotyping array. This BeadChip was developed for highly multiplexed SNP genotyping and the SNP content of this array was mainly based on findings in ankylosing spondylitis, autoimmune thyroiditis, Crohn's disease, celiac disease, IgA deficiency, multiple sclerosis, primary biliary cirrhosis, psoriasis, rheumatoid arthritis, systemic lupus erythematosus, type 1 diabetes and ulcerative colitis. Genotyping was performed according to Illumina protocols with 4 μ l of genomic DNA samples at 50ng per μ l, aliquoted to the corresponding wells of 96-well plates. The NCBI build 36 (hg19) map was used (Illumina manifest file Immuno_BeadChip_11419691_B.bpm) and normalized probe intensities were extracted for all samples passing standard laboratory quality-control thresholds. Genotype calling was performed with Illumina's GenomeStudio data analysis software, the GenomeStudio GenTrain 2.0 algorithm and the cluster file generated by Trynka *et al.* (based on the clustering of 2,000 UK samples and subsequent manual readjustment of cluster positions)³⁸.

All CVID cases from Norway, Sweden and Germany were genotyped at the Institute of Clinical Molecular Biology in Kiel, Germany. The USA/UK cases were genotyped at the Center for Applied Genomics, the Children's Hospital of Philadelphia, USA.

Quality control

Sample quality control (QC) measures included sample call rate, overall heterozygosity, relatedness testing and other metrics: Samples with a SNP call rate < 98% (n=309) as well as heterozygosity outliers (n=15), defined as beyond five standard deviation of the mean, were excluded from analysis. Duplicate samples (n=37) and cryptically related samples (PI_HAT \geq 0.1875; n=199) were identified through identity-by-state (IBS) calculations with PLINK³⁹. For each pair of duplicate or related samples the sample with the highest SNP call rate was kept in the dataset. Finally, removal of population outliers (non-Caucasians; n=101) was performed based on principal component analysis of population heterogeneity which is described below in detail as "*Principal component analysis*".

In the SNP-based QC SNPs with a call rate <98%, with a minor allele frequency < 1% and markers that deviated from Hardy-Weinberg-Equilibrium (HWE test P -value < 10^{-5}) in the controls or SNPs with significant different genotyping rate between cases and controls ($P < 1 \times 10^{-5}$ in Fisher's exact test) were removed.

Applying the QC procedures described above, resulted in 778 CVID cases and 10,999 controls available for association analysis.

Principal component analysis

Principal component analysis was conducted once to identify ethnic outliers, and once again to generate covariates to control for population stratification. For the first analysis, we used HapMap samples as reference set and 13,001 uncorrelated SNPs that passed the above QC criteria and are present in both our ImmunoChip dataset and HapMap dataset, that were LD pruned such that no pair of SNPs had $r^2 > 0.2$ and excluding problematic GC/AT SNPs and X- and Y-chromosomes. PLINK was used for LD-pruning and exclusion of SNPs. All

samples that did not cluster with the European samples were excluded. After removal of ethnicity outliers, second principal component analysis was performed within the remaining ImmunoChip samples to resolve within-Europe relationships. No population stratification in the remaining samples was observed. Principal component analyses were performed using EIGENSTRAT⁴⁰ version 4.0.

Association analysis

For case-control association testing, logistic regression with PLINK was performed using the first three principal components from the EIGENSTRAT analysis as covariates which are sufficient to control for potential population stratification as determined by the genomic inflation factor. Subphenotype analysis was similarly conducted via logistic regression. Step-wise conditional association analysis was performed by including the most strongly associated SNP in the previous step as a covariate. Post hoc power assessment showed over 99% power to detect genome-wide significant association at the HLA SNP rs1049225 (OR \approx 1.75) with 778 cases and 14 fold number of controls, and about 83% power for the *CLEC16A* SNP, rs17806056 (OR \approx 1.5)(Supplementary Fig. 8).

SNP Imputation and association testing

For the *CLEC16A* locus on chromosome 16, haplotype pre-phasing was performed using SHAPEIT^{41, 42} version 2. Genotype imputation was conducted using the IMPUTE2^{43, 44} package. The 1000 Genomes Phase I integrated variant set was used as reference panel and data were downloaded from the IMPUTE2 website (http://mathgen.stats.ox.ac.uk/impute/data_download_1000G_phase1_integrated.html). After imputation, the SNPTEST v2 package was used to perform association analysis on the imputed genotypes. Missing data likelihood score test, implemented in SNPTEST⁴³ v2, was employed to take imputation uncertainty into account. The first three principal components were included in the model as covariates. SNPs with low quality with info score < 0.8 or with HWE test *P*-value < 10⁻⁶ were excluded.

Power analysis

Power analysis was conducted using software Power for Genetic Association⁴⁵, with the following settings: Genetic Model=Co-dominant (1 df) SNP analysis; R²=1; Disease prevalence=0.00004; Marker allele frequency=Disease allele frequency=0.75; Effective degree of freedom (EDF)=123,127; alpha=0.05 and control to case ratio=14. Relative risk was set at 1.5, 1.75 and 2 to generate three power curves.

Animals

All animal studies were approved by the Institutional Animal Care and Use Committee of the Children's Hospital of Philadelphia. To generate *Clec16a*^{loxP} mice, a 15.3kb DNA fragment containing *Clec16a* exons 2–4 and flanking intronic sequence was retrieved from C57BL/6 mouse genomic DNA and subcloned into plasmid FLSniper (Ozgene) that contains an FRT-flanked PGK-driven Neomycin cassette for negative selection. One loxP site was inserted upstream of exon 3 while a second loxP site was placed downstream of exon 3. The linearized targeting vector was electroporated into B6 ES cells and clones that

survived selection were screened for homologous recombination by Southern blot analysis. Targeted clones were injected into C57BL/6-derived blastocysts that were then transferred to pseudopregnant females. Male offspring were mated to C57BL/6 females and ES cell-derived offspring were identified by PCR-based genotyping. Mice harboring the targeted insertion of the two loxP sites in the Clec16a gene locus were then crossed to the Flpo Deleter line (mouse Strain: 129S4/SvJae-Gt(ROSA)26Sortm2(FLP*)Sor/J; The Jackson Laboratory) to achieve deletion of the FRT-flanked Neomycin cassette. Clec16a^{loxP} mice were mated to UBC-Cre-ER-LBD-tg mice (inducible cre recombinase driven by the human ubiquitin C promoter) to generate UBC-Cre-Clec16a^{loxP} mice.

To generate experimental groups UBC-Cre-Clec16a^{loxP} male mice were treated with tamoxifen (for Clec16a knock down) or oil (control group). Tamoxifen (MP Biomedical) was prepared at a concentration of 20 mg/ml in 10% ethanol and 90% corn oil (Sigma). Four weeks old male mice received 1 mg of tamoxifen at 24-hour intervals for five consecutive days by gavage. Control group of mice were receiving an equal volume of corn oil alone. After tamoxifen treatment was finished, mice were aged an additional 2 weeks prior to evaluation.

Quantitative real-time PCR

The total RNA was extracted from human blood using Trizol (Ambion, Life Technologies) and converted to cDNA with High Capacity RNA-to-cDNA Kit following the manufacturer's protocols (Applied Biosystems). Briefly, 1ml of Trizol was mixed to 50µl of whole blood, followed by 200 µl of chloroform. Mix was centrifuged at 12,000×g for 15 min at 4°C. The upper aqueous phase (containing RNA) was purified with RNAeasy kit (Qiagen). Quality of RNA was assessed by Agilent Bioanalyzer. Fluorescence-based real time PCR was performed in 10µl of reaction mixture using cDNA, TaqMan Universal Master Mix and 20× FAM-MGB TaqMan assays (Applied Biosystems): Hs00322376_m1 (CLEC16A), Hs00360234_m1 (DEXI), Hs00705164_s1 (SOCS1) and Hs02758991_g1 (GAPDH). Relative gene expression was normalized to GAPDH. All PCR runs were performed on ViiA™ 7 Real Time PCR System using ViiA7 RUO software v1.2.2 (Life Technologies).

Flow cytometry

Single-cell suspensions from murine spleens (10⁶ cell per test) were stained with fluorochrome-conjugated monoclonal antibodies (mABs) in a single tube containing anti-mouse CD19-Alexa Fluor 647 (BioLegend 115522), IgD-Alexa Fluor 488 (BioLegend, 405718), IgM-Brilliant Violet 421 (BioLegend, 406517) and CD27-PE (BioLegend 124209) antibodies (1:20 dilution) for 30 min at 4°C. Cell-associated fluorescence was assessed with an LSR-II flow cytometer and analyzed using FACSDiva software (both BD). Two independent experiments were conducted, comparing the percentage of CD19+ cells (B cells) from splenocytes between inducible Clec16a knock down mice after tamoxifen treatment and the littermates treated with oil as a control. Data were combined together and B cell percentage was compared via two-sided T-test.

Naïve B cells proliferation and immunoglobulin synthesis

Naïve B cells from splenic cell suspensions were negatively selected using EasySep Mouse B cell Enrichment Kit, following the manufacturer's instructions (StemCell). Purified B cells were suspended in RPMI containing 10% FBS, L-glutamine, and 50µM β-mercaptoethanol (complete medium). For immunoglobulin (Ig) synthesis, naïve B cells (10^6 cell per ml) were cultured in complete medium alone, with LPS (20µg per ml; Sigma-Aldrich) or anti-mouse CD40 (100ng per ml; Pharmingen). Supernatants were collected after 6 days and analyzed for various Ig production by Pierce ELISA Mouse mAb Isotyping Kit, following the manufacturer's instructions (Thermo Scientific). Proliferation was measured using Cell Proliferation Kit I (MTT), following the manufacturer's instructions (Roche). For proliferation, aliquots of 10^5 B cell in 100µl of complete medium alone, or in presence LPS (20µg per ml) or anti-mouse CD40 (100ng per ml) were cultured in a 96-well flat-bottom plate for 48 hours, then the MTT labeling reagent was added to a final concentration 0.5mg per ml following by overnight incubation with the solubilization solution. Proliferation was assessed by measuring the absorbance using a microplate (ELISA) reader.

HLA analyses

Conditional analysis did not demonstrate evidence for independent association signals at the *HLA-DQBI* locus.

Imputation of classical alleles at HLA class I and II loci was performed using SNP2HLA with a reference panel consisting of 5,225 unrelated individuals collected by the Type 1 Diabetes Genetics Consortium⁴⁶.

To further explore the HLA class I and HLA class II associations with COVID, HLA allele frequencies between cases and controls at a 2-digit level were analyzed. The effect size of the association was measured with odds ratio (OR) and the confidence interval for the OR was calculated directly from the 2×2 table using the Woolf's formula⁴⁷.

Western blot analysis

For Western blot analysis, lysis of splenocytes was performed with NP40 lysis buffer (Invitrogen). Proteins were separated on 4–12% NuPAGE Bis-Tris gels in MOPS SDS running buffer and transferred overnight onto nitrocellulose membranes (Invitrogen). The membranes were blocked in 3% BSA and cut in half. The upper half of the membranes was incubated with rabbit anti-CLEC16A polyclonal antibody (Abgent, AP6983c) at 1:1000 dilution; and the lower half of the membranes was probed with mouse anti-β-Actin monoclonal antibody (Abcam, ab6276) at 1:1000 dilution. The membranes were washed, the incubated with corresponding secondary antibody for 1 hour, and washed again; bound antibody was detected with WesternBright ECL chemiluminescence detection system (Advansta). Band intensities were measured using Image J software (NIH Shareware). Representative western blot for Clec16a in splenocytes of Clec16a KD and controls mice is shown in Supplementary Fig. 9.

Supplementary Material

Refer to Web version on PubMed Central for supplementary material.

Acknowledgments

We thank David Ellinghaus, Kristian Holm and Johannes Roksund Hov for helpful discussions and analytical support, and Liv Osnes for analyzing the subphenotype flow data for the Norwegian panel. Benedicte A. Lie and The Norwegian Bone Marrow Donor Registry at Oslo University Hospital, Rikshospitalet in Oslo, as well as Matthew A Brown and Kristian Hveem are acknowledged for sharing the healthy Norwegian control data. Markus M. Nöthen is a member of the DFG Excellence Cluster “ImmunoSenstation”. This study was supported by the Southern and Eastern Norway Regional Health Authority, the German Federal Ministry of Education and Research (BMBF) grants 01EO1303 (CCI) and 01GM0896 (PID-NET) and the DZIF project TTU 04.802. This work was further supported by EU grant HEALTH-F2-2008-201549 (EURO-PADnet), an Institute Development Fund from CHOP, U01HG006830, DP3 DK085708 and a donation to CAG from the Kubert Estate Foundation. The popgen 2.0 network provided the German control data and is supported by a grant from the German Ministry for Education and Research (BMBF; ID 01EY1103). Genotyping of the European case-control collection was supported by the DFG Excellence Cluster “Inflammation at Interfaces” (EXC306, EXC306/2). This work was supported by the German Federal Ministry of Education and Research (BMBF) within the framework of the e:Med research and funding concept (grant # 01ZX1306). Stephan Brand was supported by grants from the Deutsche Forschungsgemeinschaft (DFG, BR 1912/6-1) and the Else Kröner-Fresenius-Stiftung (Else Kröner Exzellenzstipendium 2010; 2010_EKES.32). The authors are responsible for the contents of this publication.

References

1. Cunningham-Rundles C, Bodian C. Common variable immunodeficiency: clinical and immunological features of 248 patients. *Clinical immunology (Orlando, Fla)*. 1999; 92:34–48.
2. Aukrust P, et al. Persistent activation of the tumor necrosis factor system in a subgroup of patients with common variable immunodeficiency—possible immunologic and clinical consequences. *Blood*. 1996; 87:674–681. [PubMed: 8555490]
3. van Zelm MC, et al. An antibody-deficiency syndrome due to mutations in the CD19 gene. *N Engl J Med*. 2006; 354:1901–1912. [PubMed: 16672701]
4. Kuijpers TW, et al. CD20 deficiency in humans results in impaired T cell-independent antibody responses. *J Clin Invest*. 2010; 120:214–222. [PubMed: 20038800]
5. van Zelm MC, et al. CD81 gene defect in humans disrupts CD19 complex formation and leads to antibody deficiency. *J Clin Invest*. 2010; 120:1265–1274. [PubMed: 20237408]
6. Thiel J, et al. Genetic CD21 deficiency is associated with hypogammaglobulinemia. *J Allergy Clin Immunol*. 2012; 129:801–810. e806. [PubMed: 22035880]
7. Grimbacher B, et al. Homozygous loss of ICOS is associated with adult-onset common variable immunodeficiency. *Nature immunology*. 2003; 4:261–268. [PubMed: 12577056]
8. Lopez-Herrera G, et al. Deleterious mutations in LRBA are associated with a syndrome of immune deficiency and autoimmunity. *Am J Hum Genet*. 2012; 90:986–1001. [PubMed: 22608502]
9. Zhou Q, et al. A hypermorphic missense mutation in PLCG2, encoding phospholipase Cgamma2, causes a dominantly inherited autoinflammatory disease with immunodeficiency. *Am J Hum Genet*. 2012; 91:713–720. [PubMed: 23000145]
10. Salzer E, et al. B-cell deficiency and severe autoimmunity caused by deficiency of protein kinase C delta. *Blood*. 2013; 121:3112–3116. [PubMed: 23319571]
11. Salzer U, et al. Mutations in TNFRSF13B encoding TACI are associated with common variable immunodeficiency in humans. *Nature genetics*. 2005; 37:820–828. [PubMed: 16007087]
12. Vorechovsky I, et al. Family and linkage study of selective IgA deficiency and common variable immunodeficiency. *Clinical immunology and immunopathology*. 1995; 77:185–192. [PubMed: 7586726]
13. Olerup O, Smith CI, Bjorkander J, Hammarstrom L. Shared HLA class II-associated genetic susceptibility and resistance, related to the HLA-DQB1 gene, in IgA deficiency and common variable immunodeficiency. *Proceedings of the National Academy of Sciences of the United States of America*. 1992; 89:10653–10657. [PubMed: 1438261]

14. Orange JS, et al. Genome-wide association identifies diverse causes of common variable immunodeficiency. *J Allergy Clin Immunol.* 2011; 127:1360–1367. e1366. [PubMed: 21497890]
15. Parkes M, Cortes A, van Heel DA, Brown MA. Genetic insights into common pathways and complex relationships among immune-mediated diseases. *Nature reviews Genetics.* 2013; 14:661–673.
16. Su AI, et al. Large-scale analysis of the human and mouse transcriptomes. *Proceedings of the National Academy of Sciences of the United States of America.* 2002; 99:4465–4470. [PubMed: 11904358]
17. Wu C, et al. BioGPS: an extensible and customizable portal for querying and organizing gene annotation resources. *Genome Biol.* 2009; 10:R130. [PubMed: 19919682]
18. Consortium EP, et al. An integrated encyclopedia of DNA elements in the human genome. *Nature.* 2012; 489:57–74. [PubMed: 22955616]
19. Camargo JF, Lobo SA, Hsu AP, Zerbe CS, Wormser GP, Holland SM. MonoMAC syndrome in a patient with a GATA2 mutation: case report and review of the literature. *Clinical infectious diseases: an official publication of the Infectious Diseases Society of America.* 2013; 57:697–699. [PubMed: 23728141]
20. Hakonarson H, et al. A genome-wide association study identifies KIAA0350 as a type 1 diabetes gene. *Nature.* 2007; 448:591–594. [PubMed: 17632545]
21. Mells GF, et al. Genome-wide association study identifies 12 new susceptibility loci for primary biliary cirrhosis. *Nature genetics.* 2011; 43:329–332. [PubMed: 21399635]
22. Dubois PC, et al. Multiple common variants for celiac disease influencing immune gene expression. *Nature genetics.* 2010; 42:295–302. [PubMed: 20190752]
23. Hinds DA, et al. A genome-wide association meta-analysis of self-reported allergy identifies shared and allergy-specific susceptibility loci. *Nature genetics.* 2013; 45:907–911. [PubMed: 23817569]
24. Ferreira RC, et al. Association of IFIH1 and other autoimmunity risk alleles with selective IgA deficiency. *Nature genetics.* 2010; 42:777–780. [PubMed: 20694011]
25. Kim S, Waikar YP, Daniels RW, DiAntonio A. The novel endosomal membrane protein Ema interacts with the class C Vps-HOPS complex to promote endosomal maturation. *J Cell Biol.* 2010; 188:717–734. [PubMed: 20194640]
26. Kim S, Naylor SA, DiAntonio A. Drosophila Golgi membrane protein Ema promotes autophagosomal growth and function. *Proceedings of the National Academy of Sciences of the United States of America.* 2012; 109:E1072–1081. [PubMed: 22493244]
27. Zouk H, D’Hennezel E, Du X, Ounissi H, Piccirillo CA, Polychronakos C. Functional evaluation of the role of CLEC16A at the chromosome 16p13 locus. *Clin Exp Immunol.* 2011; 12:191–198.
28. Soleimanpour SA, et al. The diabetes susceptibility gene Clec16a regulates mitophagy. *Cell.* 2014; 157:1577–1590. [PubMed: 24949970]
29. Mero IL, et al. Exploring the CLEC16A gene reveals a MS-associated variant with correlation to the relative expression of CLEC16A isoforms in thymus. *Genes Immun.* 2011; 12:191–198. [PubMed: 21179112]
30. Berge T, Leikfoss I, Harbo H. From Identification to Characterization of the Multiple Sclerosis Susceptibility Gene CLEC16A. *International Journal of Molecular Sciences.* 2013; 14:4476–4497. [PubMed: 23439554]
31. Cooper JD, et al. Meta-analysis of genome-wide association study data identifies additional type 1 diabetes risk loci. *Nature genetics.* 2008; 40:1399–1401. [PubMed: 18978792]
32. Primary Immunodeficiency Diseases Report of an IUIS Scientific Committee. *Clinical & Experimental Immunology.* 1999; 118:1–28.
33. Al-Herz W, et al. Primary immunodeficiency diseases: an update on the classification from the international union of immunological societies expert committee for primary immunodeficiency. *Frontiers in immunology.* 2014; 5:162. [PubMed: 24795713]
34. Stolt P, et al. Quantification of the influence of cigarette smoking on rheumatoid arthritis: results from a population based case-control study, using incident cases. *Annals of the rheumatic diseases.* 2003; 62:835–841. [PubMed: 12922955]

35. Tsoi LC, et al. Identification of 15 new psoriasis susceptibility loci highlights the role of innate immunity. *Nature genetics*. 2012; 44:1341–1348. [PubMed: 23143594]
36. Krawczak M, Nikolaus S, von Eberstein H, Croucher PJ, El Mokhtari NE, Schreiber S. PopGen: population-based recruitment of patients and controls for the analysis of complex genotype-phenotype relationships. *Community Genet*. 2006; 9:55–61. [PubMed: 16490960]
37. Wichmann HE, Gieger C, Illig T. KORA-gen—resource for population genetics, controls and a broad spectrum of disease phenotypes. *Gesundheitswesen*. 2005; 67(Suppl 1):S26–30. [PubMed: 16032514]
38. Trynka G, et al. Dense genotyping identifies and localizes multiple common and rare variant association signals in celiac disease. *Nature genetics*. 2011; 43:1193–1201. [PubMed: 22057235]
39. Purcell S, et al. PLINK: a tool set for whole-genome association and population-based linkage analyses. *Am J Hum Genet*. 2007; 81:559–575. [PubMed: 17701901]
40. Price AL, Patterson NJ, Plenge RM, Weinblatt ME, Shadick NA, Reich D. Principal components analysis corrects for stratification in genome-wide association studies. *Nature genetics*. 2006; 38:904–909. [PubMed: 16862161]
41. Delaneau O, Marchini J, Zagury JF. A linear complexity phasing method for thousands of genomes. *Nat Methods*. 2012; 9:179–181. [PubMed: 22138821]
42. Delaneau O, Zagury JF, Marchini J. Improved whole-chromosome phasing for disease and population genetic studies. *Nat Methods*. 2013; 10:5–6. [PubMed: 23269371]
43. Marchini J, Howie B, Myers S, McVean G, Donnelly P. A new multipoint method for genome-wide association studies by imputation of genotypes. *Nature genetics*. 2007; 39:906–913. [PubMed: 17572673]
44. Howie BN, Donnelly P, Marchini J. A flexible and accurate genotype imputation method for the next generation of genome-wide association studies. *PLoS Genet*. 2009; 5:e1000529. [PubMed: 19543373]
45. Menashe I, Rosenberg PS, Chen BE. PGA: power calculator for case-control genetic association analyses. *BMC genetics*. 2008; 9:36. [PubMed: 18477402]
46. Jia X, et al. Imputing amino acid polymorphisms in human leukocyte antigens. *PLoS One*. 2013; 8:e64683. [PubMed: 23762245]
47. Kirkwood, B.; Sterne, J. *Essential medical statistics*. 2. Blackwell Science; Oxford, UK: 2003.
48. Pruim RJ, et al. LocusZoom: regional visualization of genome-wide association scan results. *Bioinformatics (Oxford, England)*. 2010; 26:2336–2337.
49. International HapMap C. The International HapMap Project. *Nature*. 2003; 426:789–796. [PubMed: 14685227]

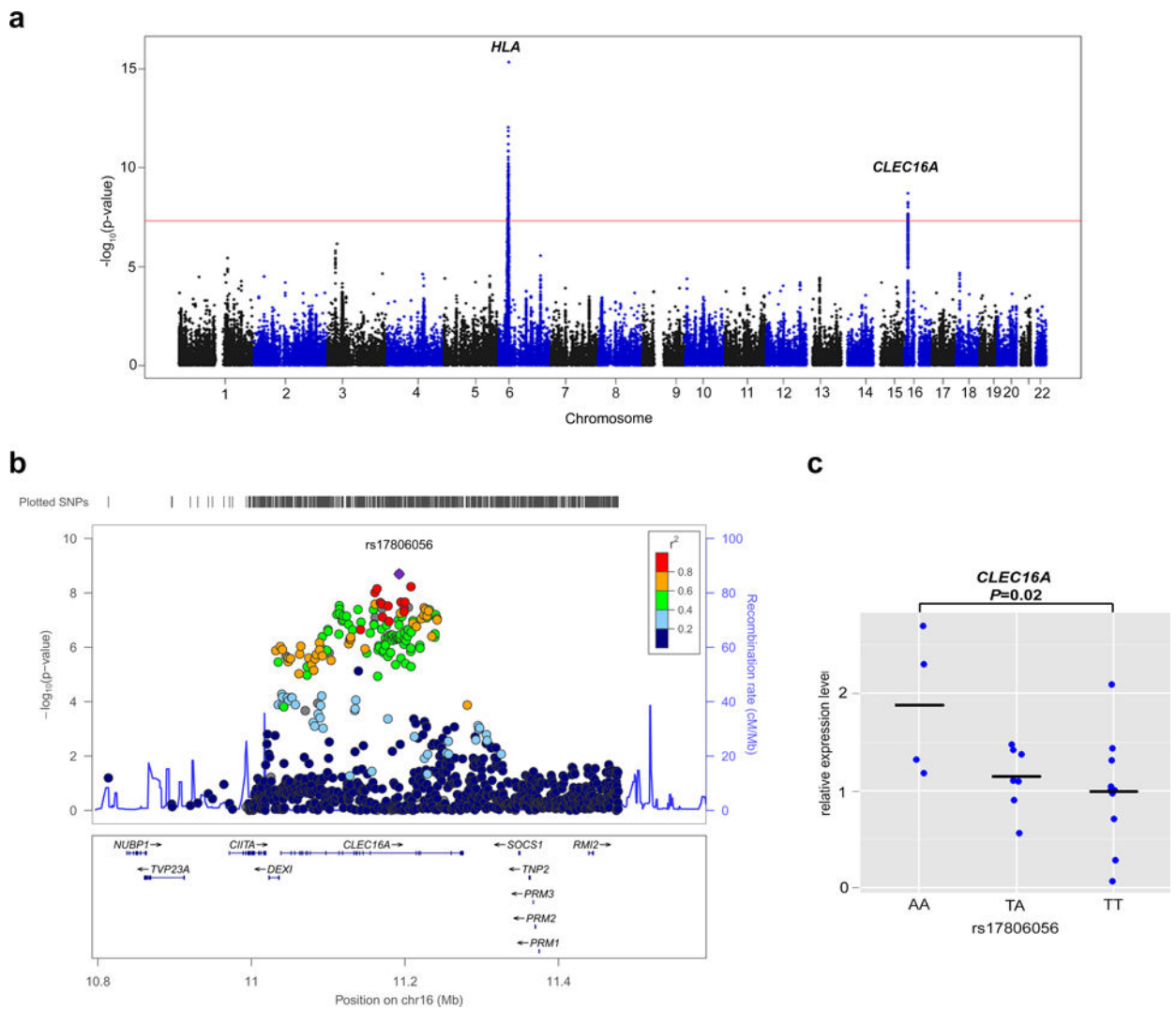


Figure 1. The association statistics for common variable immunodeficiency disorder (CVID) and the relative expression level of CLEC16A in different genotype groups

Panel a shows a Manhattan plot of the ImmunoChip association statistics illustrating CVID susceptibility loci. SNP locations are plotted on the x-axis according to their chromosomal position. The negative \log_{10} of P values per SNP derived from the association analysis are plotted on the y-axis. The horizontal red line represents the genome-wide significance threshold of $P = 5 \times 10^{-8}$. **Panel b** shows the regional association plot⁴⁸ for the *CLEC16A* locus. The most associated SNP (rs17806056) is indicated by the purple dot while the colors of the remaining SNPs indicate the linkage disequilibrium with the index SNP, as shown in the color legend. The light blue line shows the recombination rates (HapMap project⁴⁹) and genomic positions are from genome build hg19. The plot was generated using software LocusZoom⁴⁸. **Panel c** shows the relative expression level of *CLEC16A* compared between CVID cases of different genotypes at rs17806056. The mRNA level of *CLEC16A* was assessed by qRT-PCR and normalized to GAPDH control. The relative fold change (Y-axis) was plotted against the genotype for SNP rs17806056 (X-axis). Each blue dot represents the average value of three measurements from each individual sample and the black line through

the dots represents the mean level among each genotype group. The number of samples in each group is n=4 AA, n=7 TA and n=11 TT. *P*-value was determined by two-sided T-test.

Author Manuscript

Author Manuscript

Author Manuscript

Author Manuscript

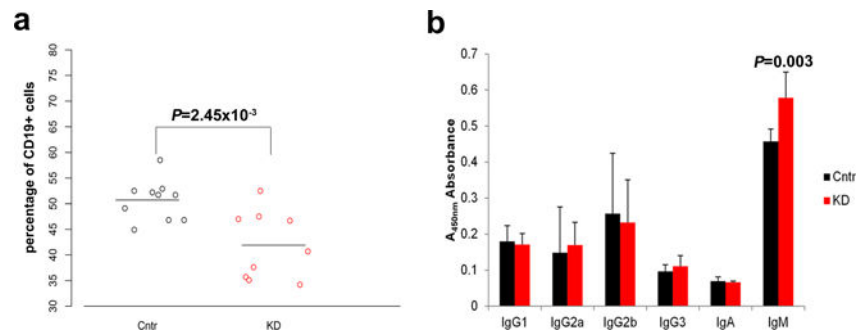


Figure 2. The effect of inducible Clec16a knockdown (KD) in murine B cells

Panel a shows the percentage of B cells (CD19⁺ cells) from splenocytes of inducible Clec16a knock down mice after tamoxifen treatment and the littermates treated with oil as a control in two independent experiments by fluorescence-activated cell sorting analysis. Data from the two experiments were combined. Black and red dots represent data from control (Cntr) and *Clec16a* knockdown (KD) mice, respectively. The black lines through the dots represent the mean level among the 10 control mice and 9 *Clec16a* KD mice respectively. Two-sided T-test was used to compare the percentage of CD19⁺ cells between *Clec16A* KD mice and control littermates. **Panel b** shows immunoglobulin production from the supernatants of B cells, purified from *Clec16A* KD mice splenocytes, cultured with anti-mouse CD40 (100ng per ml) for 6 days. Data from two independent experiments were combined. Data are mean \pm s.d. of seven mice in each group. Two-sided T-test was used to compare the level of each immunoglobulin subtype produced from *Clec16A* KD and control littermates.

Table 1

Overview of number of included patient and control panels before quality control, according to geography.

	Cases, n	Controls, n	Total, n
Sweden	93	2096	2189
Norway	112	1405	1517
USA/UK	330	1402	1732
Germany	351	6649	7000
Total	886	11552	12438

Author Manuscript

Author Manuscript

Author Manuscript

Author Manuscript

Genome-wide significant ($P < 5 \times 10^{-8}$) associations detected by logistic regression analysis of 778 cases with common variable immunodeficiency disorder and 10,999 population controls.

Table 2

SNP ^a	Chr.	Position (hg19)	A1/A2	MAF cases/controls	OR (95% CI)	P-value	Candidate gene	Additional SNPs ^b
rs1049225	6p21	32,627,747	A/G	0.16/0.26	0.56 (0.49, 0.64)	4.8×10^{-16}	<i>HLA-DQB1</i>	154
rs17806056	16p13.13	11,192,499	A/T	0.18/0.23	0.66 (0.57, 0.75)	2.0×10^{-9}	<i>CLEC16A</i>	21

SNP, single nucleotide polymorphism; Chr, chromosome; A1, minor allele; A2, major allele; MAF, minor allele frequency; OR, odds ratio; CI, confidence interval.

^aMost associated SNP from each locus.

^bNumber of additional genome-wide associated SNPs at the respective loci